





This is the peer reviewed version of the following article: Mahmood T., Wittenberg, P., Zwetsloot, I.M., Wang, H., Tsui, K.L. (2019). Monitoring data quality for telehealth systems in the presence of missing data. *International Journal of Medical Informatics* 126, 156–163, which has been published in final form at <https://dx.doi.org/10.1016/j.ijmedinf.2019.03.011>. This manuscript version is made available under the [CC-BY-NC-ND 4.0](https://creativecommons.org/licenses/by-nc-nd/4.0/) license.

Monitoring data quality for telehealth systems in the presence of missing data

Tahir Mahmood,^{a,1}  Philipp Wittenberg,^{b,1}  Inez Maria Zwetsloot,^{a,c,1,*}  Hailiang Wang,^c and Kwok Leung Tsui^c 

^aDepartment of System Engineering and Engineering Management, City University of Hong Kong, Tat Chee Avenue, Kowloon, Hong Kong

^bDepartment of Mathematics and Statistics, Helmut Schmidt University, Hamburg, Germany

^cSchool of Data Science, City University of Hong Kong, Tat Chee Avenue, Kowloon, Hong Kong

*Corresponding author: i.m.zwetsloot@cityu.edu.hk

¹Authors contributed equally

Abstract

Background: All-in-one station-based health monitoring devices are implemented in elder homes in Hong Kong to support the monitoring of vital signs of the elderly. During a pilot study, it was discovered that the systolic blood pressure was incorrectly measured during multiple weeks. A real-time solution was needed to identify future data quality issues as soon as possible.

Methods: Control charts are an effective tool for real-time monitoring and signaling issues (changes) in data. In this study, as in other healthcare applications, many observations are missing. Few methods are available for monitoring data with missing observations. A data quality monitoring method is developed to signal issues with the accuracy of the collected data quickly. This method has the ability to deal with missing observations. A Hotelling's T-squared control chart is selected as the basis for our proposed method.

Findings: The proposed method is retrospectively validated on a case study with a known measurement error in the systolic blood pressure measurements. The method is able to adequately detect this data quality problem. The proposed method was integrated into a personalized telehealth monitoring system and prospectively implemented in a second case study. It was found that the proposed scheme supports the control of data quality.

Conclusions: Data quality is an important issue and control charts are useful for real-time monitoring of data quality. However, these charts must be adjusted to account for missing data that often occur in healthcare context.

Key words: Data quality; elderly; multivariate control charts; statistical quality control; vital sign monitoring

1 Background

Applications of Telehealth are growing due to the fast development of sensor technology. This has enabled the development of relatively cheap and easy-to-use devices for (self-)evaluation of health indicators and well-being. These techniques have the potential to help current elder care providers to track vital signs, detect physiological changes and predict health risks.

A pilot study has been conducted with an all-in-one station-based telehealth device in Hong Kong to help track elder's vital signs. This telehealth system is designed to provide computer-aided decision support for clinicians and community nurses. It also enables them to easily monitor and analyze an elder's vital signs and well-being. For more details on this system see Yu and colleagues [1]. The present study involved two elder care centers. In each center, elder's volunteered to have their vital signs measured daily. For approximately three months, trained and qualified research staff visited the centers and assisted the elders to accomplish

the measurements on each measurement day (usually five days a week). Vital signs were measured using a commercial all-in-one station-based telehealth device (TeleMedCare, Health Monitor, TeleMedCare, Sydney, Australia). Data is stored on a server, processed, analyzed and summarized into a report which is given to the participants. The framework of this telehealth monitoring system is shown in the top panel of Fig. 1.

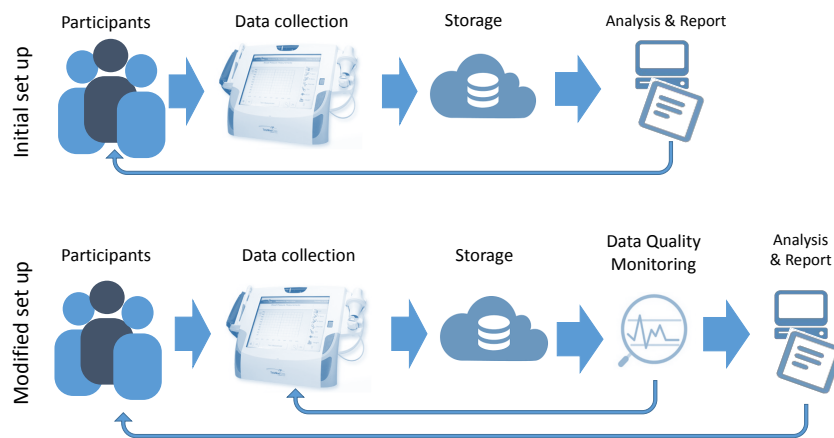


Figure 1. Overview of the telehealth system, initial (top) and modified (bottom).

In the pilot study, we found that the systolic blood pressure was incorrectly recorded during multiple weeks. A structural data quality method was needed to ensure the accuracy of vital signs data collection. The proposed data quality monitoring is implemented on a daily basis with a feedback loop to the telehealth monitoring system, as illustrated in the lower panel of Fig. 1.

2 Methods

2.1 Settings

The elder care center where the systolic blood pressure was incorrectly measured (center A), is an elder day care center situated in Kowloon, Hong Kong. The pilot study in center A had 24 participants and was conducted in a period from 18.12.2017 to 07.03.2018. For each participant, five vital signs were measured on each measurement day; body temperature (BT) in degrees Celsius ($^{\circ}\text{C}$), systolic and diastolic blood pressure (SBP and DBP) in millimeters of mercury (mm Hg), heart rate (HR) in number of beats per minute and peripheral capillary oxygen saturation (SpO_2) in percentages (%). We also included a second center (B) in our pilot study. In center B there were 12 participants and the study ran from 01.03.2018 to 31.05.2018.

Fig. 2 gives an overview of the collected data, with the panels showing the vital signs for all participants in center A (left) and center B (right) over the entire study period. Note that initial data is cleaned by deleting improbable low values (i.e. outliers such as HR values of zero).

Close evaluation of Fig. 2 showed that starting from 12.02.2018 the SBP measurements in Center A do not exceed 136, which is an abnormally low maximum value for SBP measurements. Retrospective investigation revealed that the SBP measurement subsystem was accidentally and unknowingly limited to a maximum value of 136. Hence, the collected data was capped for the rest of the study period. This data quality issue affected all study participants in center A.

2.2 Choice of solution

In industrial applications, measurement system analysis (MSA) is performed to verify the accuracy of the measurement system. MSA studies evaluate the repeatability and reproducibility of the measurement system. And focus on the measurement system as a whole, including the measurement device, the people operating the device as well as the environment [2]. A control chart is an associated tool often used to visualize measurement variability. In this paper, a data quality monitoring method based on a control chart is proposed to improve the measurement accuracy of the data collected with the telehealth device.

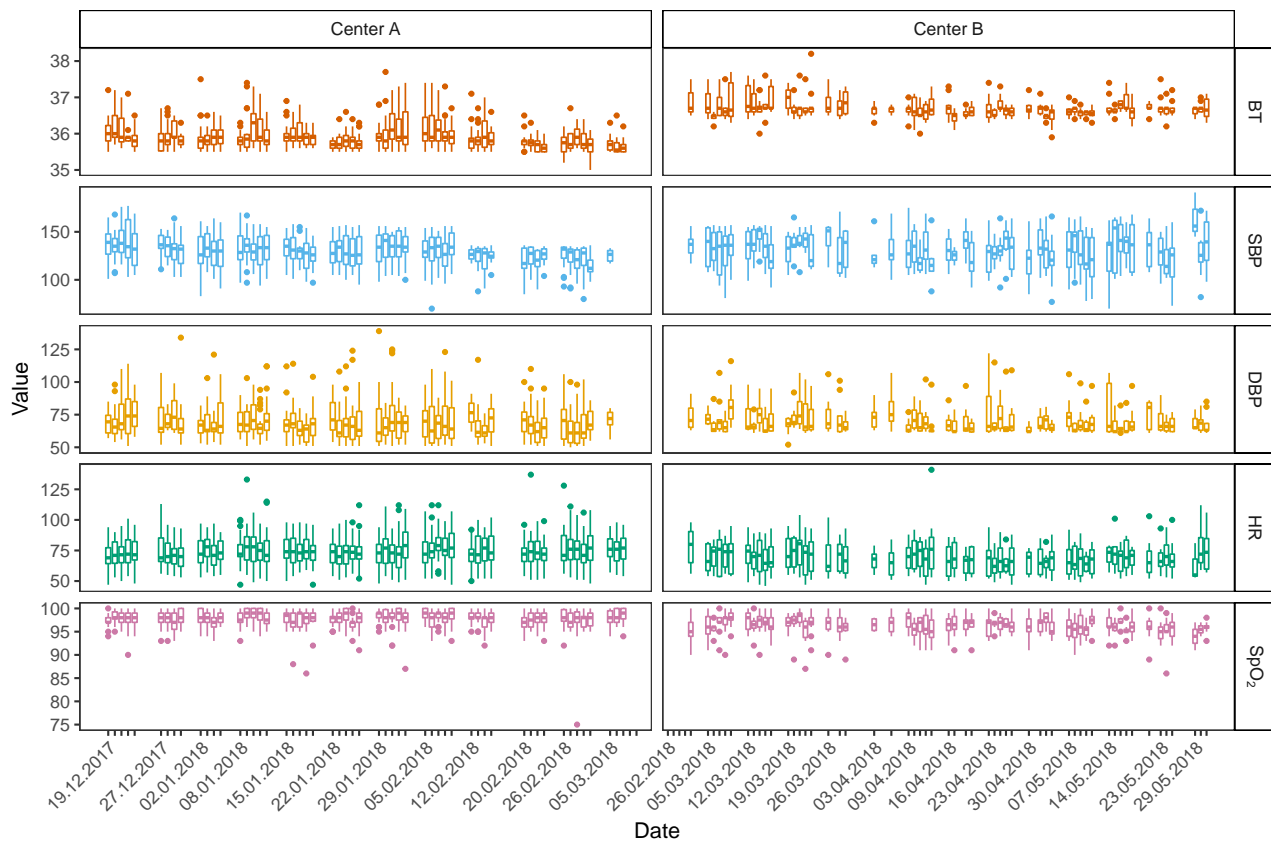


Figure 2. Boxplots of vital signs for elders in center A (left panel) and B (right panel).

A control chart is a statistical and visual tool. It is designed to prospectively signal change(s) in data streams quickly. Control charts have been used in clinical settings [3], as well as for monitoring the quality of cardiac surgery [4] and for monitoring in epidemiologic studies [5]. Overviews of control charts in healthcare settings can be found in [6–8]. More specifically, single patient univariate and multivariate monitoring of vital signs is done in [9] who used deleted cases. Cornélissen and colleagues [10] implement self-starting CUSUM chart for vital signs monitoring. Sparks and colleagues [11] monitor vital sign trends of a single patient with univariate exponential weighted moving average control charts and multiple vital signs with dynamic Biplots.

A control chart can also be used to monitor data quality by detecting changes in the data collection system as timely as possible. Jones-Farmer and colleagues [12] provide a framework for control charts and data quality monitoring. An error in the measurement system will show up as a change in the level of the vital sign(s). Hence, a change in the level of vital sign(s) should be signaled.

A standard method used to monitor multiple variables is the Hotelling’s T -squared control chart, for example see [3, 13]. As our all-in-one station-based telehealth device records multiple vital signs for each participant we employed a Hotelling’s T -squared control chart. The choice for a multivariate, rather than multiple univariate charts is motivated medically as vital signs are known to be correlated, for example SBP and DBP [14]. In section 3 we verify this when we implement our case studies.

Each day we obtain data from multiple participants consecutively. In this work, we choose to treat the data as grouped and obtain each day a data matrix containing all vectors of each individual (see section 2.4 for details). We have three reasons to adopt this approach, rather than treating the data as individual data. Firstly, it fits with the nature of our data collection: the data collected with the telehealth device were synchronized daily after all participants have undergone the measurements. Secondly, subgrouping our data helps with the missing data issue. We create from the subgrouped data a vector of averages. Hence a matrix with a lot of missing data is converted to a vector which is nearly always complete (see section 2.4 for details). Thirdly, by subgrouping and averaging our data we create approximately independent and normally distributed data. Finally, this leads to the convenience of monitoring a single control chart rather than one chart for each participant.

2.3 Missing data

In observational studies missing data are often encountered (cf. [15]) and our study is no exception. We encounter three types of missing data:

1. Not every vital sign is obtained daily.
2. Due to the type of elder care centers (day care) not all elders show up everyday for measurements.
3. Some elders join the program late or drop out early. Resulting into a long streams of missing data at the start or end of the study period, which is a common situation in healthcare related studies [16].

Fig. 3 displays the varying number of obtained measurements (elders) over time for each vital sign and center. This varying sample size shows that we have many missing data (without missing data all sample sizes would be equal to 24 of center A and 12 for center B). Overall 10.3 % of the data is missing in center A. This percentage varies across the vital signs from 1.7% up to 14.3%. Overall 3.9% of the data is missing in center B. The percentage varies across the vital signs from 2.4% up to 6.3%.

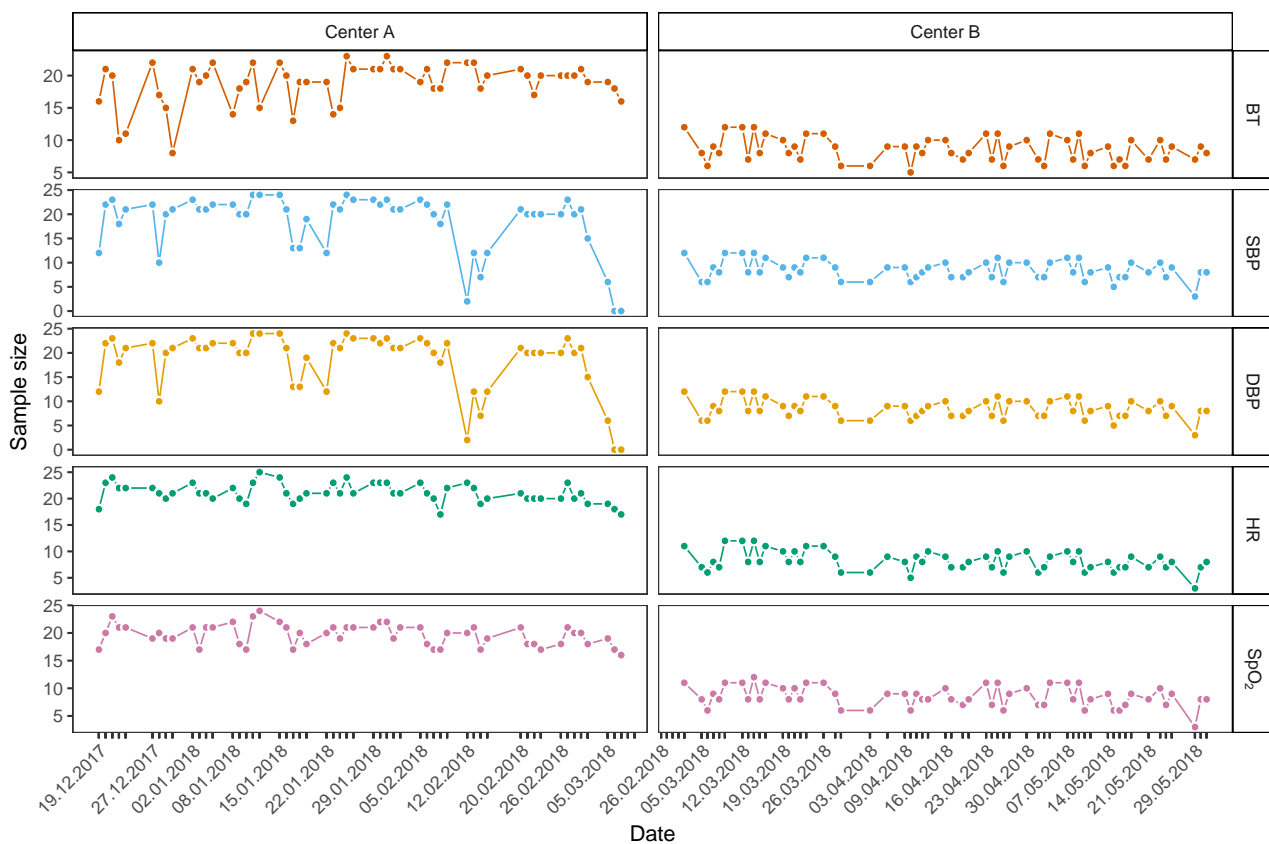


Figure 3. Sample size of vital signs for elders in center A (left panel) and B (right panel).

The literature [17] categorizes random missing data into two types: missing at random (MAR) and missing completely at random (MCAR). The propensity of the MAR observations is due to the random in-out of the elders and machining problems while observations in the data set are MCAR when a random event (e.g., typhoon) occurred and it is independent of the machining problems and presence of elders. From the available information, it is assumed that the data is missing at random (MAR) in our study.

Traditional control charts are designed for complete data sets and it is difficult to run charts with missing data. A solution to apply control charts to our incomplete dataset (addressed above as first type of missing data) with varying number of elders on each time point (afore-mentioned missing data type two and three) is needed. One way to deal with missing data, in a healthcare setting, is to perform data imputation to “fill in” the missing values. This approach is taken by [3] for the multivariate monitoring in a clinical setting and by [18] who use imputation in a longitudinal study. The effect of using different imputation methods on the performance of multivariate control charts is studied by [19] and [20]. Both studies concluded that control

charts based on imputation methods provide better performance as compared to control charts based on deletion method. Currently, imputation is the selected method when missing observations are encountered. However, [21] showed that imputation can only work properly when the percentage of missing data is small and when we know this percentage a-priori. For our settings, data imputation is complicated because of the afore-mentioned third type of missing data: late joining and dropping of elders. This is uncontrollable and the number of late joiners is unknown a-priori. Therefore, it is unknown a-priori what the percentage of missing data will be.

Another way to deal with missing data is to use control charts for variable sample sizes (i.e. varying number of participants per day). Previous studies proposed some methods for univariate data [22, 23] and some for multivariate data [24, 25]. The latter methods assume that the varying sample sizes are known a-priori and that the researcher controls the number of samples. Hence these methods are not straightforward applicable here.

To the best of our knowledge, none of the existing control charts for variable sample sizes has the ability to adequately deal with random varying sample sizes in a multivariate setting. Hence, a new method is developed by adapting the Hotelling’s T -squared control chart to accommodate for missing data and random varying sample size without the need to impute missing data.

2.4 Method development

For the purpose of method development, each participant is indexed by k ($k = 1, 2, \dots, n$), each vital sign by j ($j = 1, 2, \dots, p$) and each day by i . Let X_{ijk} be the measurement of person k for vital sign j on day i . Hence, n vectors $\mathbf{X}_{ik} \in \mathbb{R}^p$ are obtained each day. Let $\boldsymbol{\mu}$ denote the expectation and $\boldsymbol{\Sigma}$ the covariance matrix of \mathbf{X}_{ik}

To monitor the data quality, the average value for each vital sign is computed by averaging over those patients who showed up for measurement on day i . Giving vector $\bar{\mathbf{X}}_i$ of p elements $(\bar{X}_{i1}, \dots, \bar{X}_{ip})^\top$. Here, \bar{X}_{ij} is the average of $n_{ij} \leq n$ elders for vital sign j . The number of elders n_{ij} depends on the day i and the vital sign j , and the changing n_{ij} allow us to model the missing data (n_{ij}). In Table 1 we show the data structure, in this example elder #2 did not show up and therefore its data is missing as indicated by a star. Also the first vital sign for elder #1 was not recorded. The right column shows the corresponding sample sizes for each vital sign in this example, the actual values of n_{ij} are displayed in Fig. 3.

Table 1. Data structure, missing data indicated by a *.

\mathbf{X}_{i1}	\mathbf{X}_{i2}	\mathbf{X}_{i3}	\dots	\mathbf{X}_{ik}	\dots	\mathbf{X}_{in}	\rightarrow	$\bar{\mathbf{X}}_i$	\mathbf{n}_i
*	*	X_{i13}	\dots	X_{i1k}	\dots	X_{i1n}	\rightarrow	\bar{X}_{i1}	n_{i1}
X_{i21}	*	X_{i23}	\dots	X_{i2k}	\dots	X_{i2n}	\rightarrow	\bar{X}_{i2}	n_{i2}
\vdots	\vdots	\vdots	\vdots	\vdots	\vdots	\vdots	\vdots	\vdots	\vdots
X_{ip1}	*	X_{ip3}	\dots	X_{ipk}	\dots	X_{ipn}	\rightarrow	\bar{X}_{ip}	n_{ip}

In section 2.3, we argued that our data is MAR. Under this MAR assumption it follows that $\boldsymbol{\mu}_{\bar{\mathbf{X}}} = \boldsymbol{\mu}$ and after some derivation (see Appendix), we also have

$$\boldsymbol{\Sigma}_{\bar{\mathbf{X}}_i} = \mathbf{W}_i \odot \boldsymbol{\Sigma}. \tag{1}$$

Here, \odot denotes element wise matrix multiplication, which is also known as Hadamard multiplication and \mathbf{W}_i is a matrix weighting the elements of $\boldsymbol{\Sigma}$ according to the number of paired observations (participants) available for measurement on day i . The matrix \mathbf{W}_i is a $p \times p$ matrix defined as

$$\mathbf{W}_i = \left[\frac{|U_{ij} \cap U_{ij'}|}{n_{ij}n_{ij'}} \right]_{j,j'=1,\dots,p}. \tag{2}$$

Here, U_{ij} is the set of participants for whom a measurement of vital sign j on day i is available and $n_{ij} = |U_{ij}|$ is the number of elements in U_{ij} , i.e. the number of participants. For example, if on day i two participants, say #1 and #3, showed up to measure vital sign $j = 2$ then $U_{i2} = \{1, 3\}$ and $n_{i2} = 2$. Note that under

complete observations, it follows that $n_{ij} = n$ and hence $\mathbf{W}_i = [1/n]$. It is possible that $n_{ij} = 0$ when one of the vital signs j is not measured for all participants on the day i . This happened on the final two days in center A for SBP and DBP. To account for this we reduce the dimension of our monitoring statistic. This will be discussed in detail below.

The design of a Hotelling's T -squared monitoring statistic is $T_i^2 = (\bar{\mathbf{X}}_i - \boldsymbol{\mu})^\top \boldsymbol{\Sigma}_{\bar{\mathbf{X}}_i}^{-1} (\bar{\mathbf{X}}_i - \boldsymbol{\mu})$. In order to compute this statistic, estimates of the unknown parameters $\boldsymbol{\mu}$ and $\boldsymbol{\Sigma}_{\bar{\mathbf{X}}_i}$ are needed. For this we select the first 19 days from each study for estimation (as the Phase I data set). To avoid biased estimates due to outliers in the data (see Fig. 2), estimates of the mean vector $\hat{\boldsymbol{\mu}}$ and the covariance matrix $\hat{\boldsymbol{\Sigma}}$ are obtained using a robust estimation method. Various robust methods have been evaluated [26] for the Hotelling's T -squared control chart. Here, the orthogonalized Gnanadesikan–Kettenring (OGK) estimation method [27] is used, because it provides positive definite and approximately affine equivariant robust estimates. The OGK estimators are obtained using the R-package `rrcov` [28]. Recall that $\hat{\boldsymbol{\Sigma}}_{\bar{\mathbf{X}}_i} = \mathbf{W}_i \odot \hat{\boldsymbol{\Sigma}}$ by using the OGK estimator we obtain $\hat{\boldsymbol{\Sigma}}$ based on the Phase I data which we clubbed and omitted incomplete cases. We argued that the data are missing MAR, therefore this should yield a unbiased and consistent estimator of $\boldsymbol{\Sigma}$ and hence also of $\boldsymbol{\Sigma}_{\bar{\mathbf{X}}_i}$.

The final monitoring statistic now becomes:

$$T_i^2 = (\bar{\mathbf{X}}_i - \hat{\boldsymbol{\mu}})^\top (\mathbf{W}_i \odot \hat{\boldsymbol{\Sigma}})^{-1} (\bar{\mathbf{X}}_i - \hat{\boldsymbol{\mu}}) \quad (3)$$

and the control chart signals, when T_i^2 exceeds the Upper Control Limit (UCL). Whenever T_i^2 exceeds the UCL, a signal is observed. This signal should be investigated and appropriate corrective action should be taken. Usually, for multivariate control charts, a decomposition method is used to determine which variables are responsible for the signal. For our proposed Hotelling's T -squared control chart, the Mason-Young-Tracy (MYT) decomposition method [29] was adopted. In the MYT decomposition, T^2 statistics are calculated for all possible subsets of vital signs and plotted against the respective UCL to identify the vital sign or combination of vital signs, which give a signal.

The UCLs for all possible combinations of vital signs are obtained by using the following simulation procedure:

1. Generate a data set of $m \times \bar{n}$ vectors $\mathbf{X}_i \sim \mathcal{N}(\hat{\boldsymbol{\mu}}, \hat{\boldsymbol{\Sigma}})$. Here m represents the number of days of data used to estimate the mean and covariance. And $\bar{n} = \frac{1}{mp} \sum_{i=1}^m \sum_{j=1}^p n_{ij}$ is defined as the overall average number measurements for the vital signs obtained on a day.
2. Based on this data set, compute the robust mean vector $\hat{\boldsymbol{\mu}}_{\text{OGK}}$ and covariance matrix $\hat{\boldsymbol{\Sigma}}_{\text{OGK}}$ by using the OGK estimation method.
3. Generate vector $\bar{\mathbf{X}}_i \sim \mathcal{N}(\hat{\boldsymbol{\mu}}, \hat{\boldsymbol{\Sigma}}/\bar{n})$. Compute the Hotelling's T -squared statistic as $T_i^2 = (\bar{\mathbf{X}}_i - \hat{\boldsymbol{\mu}}_{\text{OGK}})^\top \hat{\boldsymbol{\Sigma}}_{\text{OGK}}^{-1} (\bar{\mathbf{X}}_i - \hat{\boldsymbol{\mu}}_{\text{OGK}})$.
4. Repeat step 3 for 10,000 times and select the $(1 - \alpha)$ -th quantile of T^2 as UCL.

Repeat steps 1-4, 100 times and calculate the final UCL as the average of all obtained control limits from step 4. For both center A and B, m equals 19. For center A \bar{n} equals 20 and for center B \bar{n} equals 9. From the simulations, we get UCL = 17.31 for center A and UCL = 18.59 for the center B. These UCLs are obtained by fixing the false alarm rate $\alpha = 0.02$, which implies a false alarm every 50 days on average. To obtain these UCLs, we have assumed complete data in our simulation procedure. This is a simplification to facilitate easy simulation. We have also implemented the simulation procedure with varying missing data scenarios. The obtained UCLs for these scenarios are all comparable to the limits discussed above and they differ maximally at a level of 5%.

One additional modification to the chart (reduction in vital signs) is necessary. Whenever a vital sign is not measured for at least one participant, one element in $\bar{\mathbf{X}}_i$ will be missing. The corresponding row from $(\bar{\mathbf{X}}_i - \boldsymbol{\mu})$ is then removed, the corresponding row and column from $\boldsymbol{\Sigma}_{\bar{\mathbf{X}}_i}$ are also removed and finally, the control limit is adjusted for that time instance. For example, in center A, only three vital signs are measured on the last two days of the study (see Fig. 3), so a reduced UCL is plotted at 13.29.

Finally, before this chart can be implemented, it is important to verify that the data comply with the important underlying assumptions of our method. In this study, it is assumed that the average vector $\bar{\mathbf{X}}_i$

follows a multivariate independent normal distribution with a mean vector $\mu_{\bar{x}_i}$ and covariance matrix $\Sigma_{\bar{x}_i}$. Note that we assume normality for the average, this is rather convenient, as vital signs will not be normally distributed on an individual basis. However for mean vectors we can expect that normality is a reasonable assumption. We verify this assumption by performing several multivariate normality tests; Mardia's test [30] and Henze-Zirkler's multivariate normality test [31] implemented in the R-package MVN [32]. Next we need to consider independence. It is known that vital signs show autocorrelation [33]. For our application we consider the average vector, any autocorrelation in the individual vital signs will decline by averaging over observations. We verify that the average vector is approximately independent over time using the standard acf function in R. A third important step we take is the estimation of our μ and Σ matrix. We use the robust OGK estimator using clubbed complete cases data for the first 19 days. Here we assume that this estimator is unbiased and consistent even though we use a subset of data. It is difficult to check this empirically, however the authors [27] of the OGK estimator state in their paper that this estimator is robust to various types of outliers. Ideally we would prefer an Phase I estimator that is also shown to be robust to missing data and deviations from normality. However, to our knowledge an estimator for the variance-covariance matrix that can handle outliers, missing data as well as slight deviations from normality in sub grouped data does not (yet) exist. We welcome new research on this issue. We compared all existing estimations methods and from both a empirical as well as theoretical point of view we believe the OGK estimator served our purpose best.

3 Findings

Our control chart is designed to detect data quality issues. A signal may show that the SBP measurement sub-system is capped (the reason for this project). However, a signal can also be caused by changes in individual participant's vital signs. This signal than may point towards the need for medical assistance (rather than measurement system calibration). In the elder care centers, well trained personal takes care of the elders. In this project, we consulted with them after any signal caused by individual vital sign levels. A separate project is being conducted to design a monitoring system for individuals. However, before we can monitor individual's vital signs for changes in health, we need to ensure that the collected data is accurate. That is where our proposed method is applied. The proposed monitoring method is first validated on center A and next prospectively run on center B to monitor the data quality.

3.1 Retrospective implementation for center A

Next the proposed method is retrospectively implemented for center A. The first 19 days, from 19.12.2017 to 16.01.2018, are used to obtain the OGK estimates:

$$\hat{\mu} = \begin{pmatrix} \hat{\mu}_{BT} \\ \hat{\mu}_{SBP} \\ \hat{\mu}_{DBP} \\ \hat{\mu}_{HR} \\ \hat{\mu}_{SpO_2} \end{pmatrix} = \begin{pmatrix} 35.93 \\ 131.31 \\ 67.55 \\ 73.38 \\ 97.94 \end{pmatrix}$$

and

$$\hat{\Sigma} = \begin{bmatrix} 0.10 & -0.01 & -0.06 & 0.28 & 0.00 \\ -0.01 & 254.92 & 22.33 & -48.58 & 0.56 \\ -0.06 & 22.33 & 87.13 & 3.54 & -0.04 \\ 0.28 & -48.58 & 3.54 & 130.38 & 5.18 \\ 0.00 & 0.56 & -0.04 & 5.18 & 2.36 \end{bmatrix}.$$

Before we plot the proposed control chart, we validate the most important assumptions of normality and independence over time. We also study the correlation between the vital signs to motivate the multivariate nature of our method. We found no evidence of deviation from multivariate normality. In addition we compute the autocorrelation function and found no evidence of significant autocorrelation between the mean levels of each of the vital signs. Finally, we looked at the correlation matrix, standardized from the variance-covariance matrix above, and concluded that multiple pairs of vital signs are correlated as validated by Bartlett's test of sphericity [34] (p-value < 0.0001).

Next, the control chart is plotted to monitor the data quality in case A. The Hotelling's T -squared statistics are calculated by using Equation (3) and plotted against the UCL=17.31 in Fig. 4.

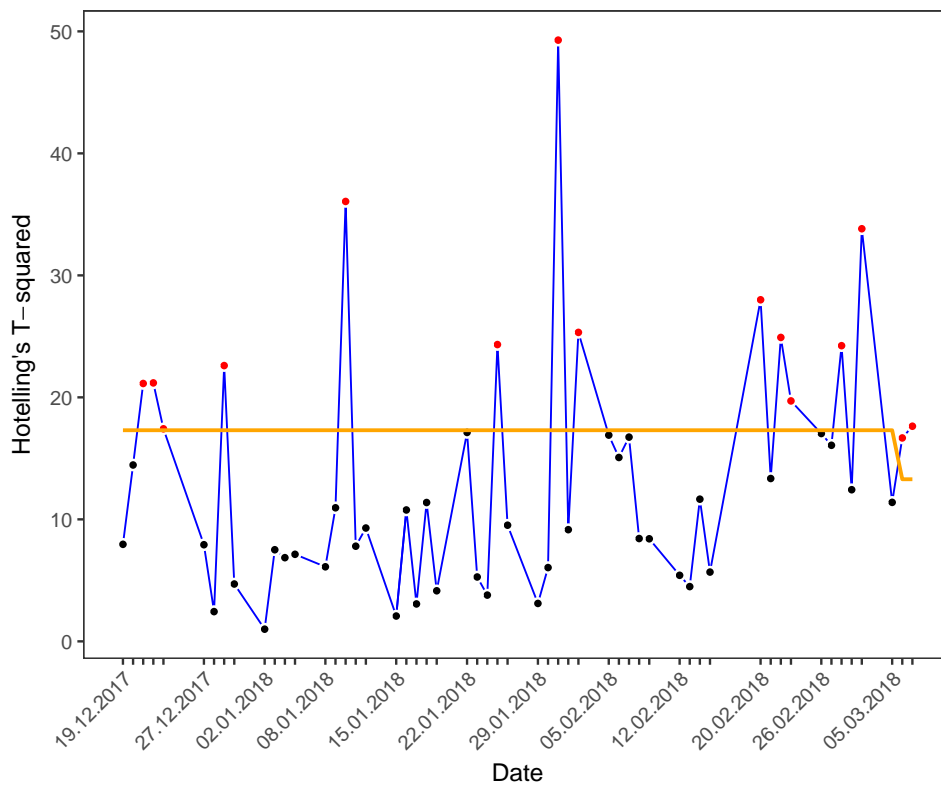


Figure 4. Hotelling's T -squared chart for center A.

The following catches the eye:

- The first four signals are observed in the interval from 21.12.2017 to 29.12.2017. The MYT decomposition method identifies all signals as caused by changes in the mean of the DBP measurements.
- The next four signals are observed in the interval from 10.01.2018 to 02.02.2018. MYT decomposition method classifies the 5th, and 7th signal as driven by variation in the DBP and BT measurements. The 6th signal, on 25.01.2018, is due to the variation in SpO₂ measurements. The 8th signal, on 02.02.2018, is due to variation in DBP.
- The signals from 20.02.2018 until 02.03.2018 were expected as these signals are due to the capped measurements of SBP. However, the signal is delayed by four days. The MYT decomposition indicates that apart from SBP the BT also influenced the signal.
- In the last two days, two signals are observed. The MYT decomposition indicated a decrease in the means of the BT measurements.

Overall, the collected data are not stable in this pilot study. Many issues, especially with the SBP measurement are discovered. Hence, it is necessary to implement a data quality monitoring method into the telehealth system (Fig. 1). Such a method can help to detect undesirable situation as soon as possible so that appropriate action can be taken. Apart from the monitoring scheme, other actions such as training of staff and standardized working procedures were also applied to ensure repeatable and reproducible measurements.

3.2 Prospective implementation for center B

To evaluate the usefulness of our developed Hotelling's T -squared control chart, we prospectively implement the developed control chart for center B. Thereby, we verify in real-time, whether the telehealth system is functioning normally. The data collection started on 02.03.2018 and the first week of observations are used to

estimate the parameters ($\hat{\mu}$ and $\hat{\Sigma}$). A signal was observed on 09.03.2018, after careful investigation and MYT decomposition, it was discovered that the DBP measurements were set to a maximum level on that day. This issue was solved by adjusting the telehealth device.

The data collection was continued in the subsequent weeks and the Hotelling's T -squared control chart, based on re-estimated parameters was plotted. This iterative method was continued until $m = 19$ days of data were collected. The corresponding OGK estimates for the mean vector and covariance matrix are

$$\hat{\mu} = \begin{pmatrix} \hat{\mu}_{BT} \\ \hat{\mu}_{SBP} \\ \hat{\mu}_{DBP} \\ \hat{\mu}_{HR} \\ \hat{\mu}_{SpO_2} \end{pmatrix} = \begin{pmatrix} 36.83 \\ 133.96 \\ 69.80 \\ 71.11 \\ 96.96 \end{pmatrix}$$

and

$$\hat{\Sigma} = \begin{bmatrix} 0.12 & 0.90 & -0.06 & 0.55 & 0.23 \\ 0.90 & 328.42 & 29.28 & 60.74 & 5.59 \\ -0.06 & 29.28 & 69.99 & 27.13 & -0.39 \\ 0.55 & 60.74 & 27.13 & 184.52 & 0.29 \\ 0.23 & 5.59 & -0.39 & 0.29 & 3.34 \end{bmatrix}.$$

Similarly, as in Case A, we have validated assumptions; we found no statistical significant difference from normality nor any evidence for autocorrelation. Furthermore, some pairs of vital signs show correlation (Bartlett's test p -value < 0.0001). The Hotelling's T -squared control chart for the full study period is displayed in Fig. 5.

A second signal was observed on 13.04.2018, after careful investigation the signal can be attributed to a very high HR for a single participant. Another signal was observed on 29.05.2018, the MYT decomposition method identified that the cause for the signal is an unusual high SBP level and an unusual low SpO_2 level.

Overall, the implementation of the data quality monitoring method provides a timely indication of data quality issues which may leads to adjustment of the telehealth system and a decrease in the wastage of resources.

4 Discussion and conclusion

Telehealth applications provide many opportunities for innovations in healthcare. However, the accuracy and reliability of measured data may be challenging to guarantee when various people, especially non-medical experts, perform the measurements [35–37]. There are many ways to validate and guarantee data accuracy, such as training people and calibration of the measurement system. In this article, we set forth an additional check to verify the real-time quality of measured data. A Hotelling's T -squared control chart is designed, which is modified to deal with missing data. After testing the proposed method on a case study with known data quality issues, the control chart is prospectively implemented on a second case study. In the second study, a data quality issue is detected after one week, which was timely solved. Hence, a regular focus on the data quality helps to ensure the validity and accuracy of the collected measurements and a quick feedback to the data quality monitoring system is essential to solve problems on-time.

Data monitoring is also important on an individual level and more comprehensive models are needed to deal with the heterogeneity of individuals. An individual monitoring tool can be helpful to detect health changes for each elder separately. However, before this can be done, the data has to be accurate. The developed method for data quality monitoring can thus be seen as a first step before monitoring the health individually. The focus is on handling the variable sample sizes, in our application due to MAR type missing data. Our approach can also be applied to other scenarios with missing data where monitoring is required. It would be useful if future research would compare the proposed method to existing methods for monitoring data with missing observations, such as the imputation method.

EWMA or CUSUM control charts are generally quicker in detection of a failure mode than a Hotelling's T -squared control chart. Therefore, a possible extension for future research could be a multivariate version of the CUSUM procedure with the dynamic probability control limits developed by [22].

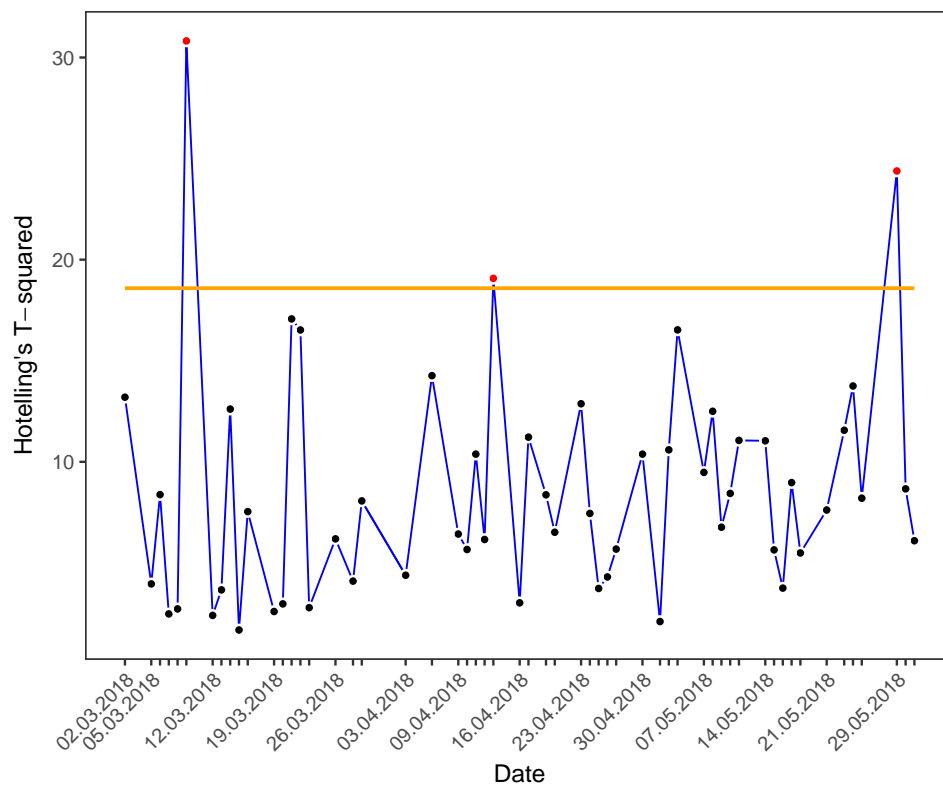


Figure 5. Hotelling's T -squared chart for center B.

Author contributions

All authors made substantial contributions to the study design and methods. HW, KLT and IZ extracted data. PW, TM and IZ analyzed and visualized the data and derived the method. Further, all authors interpreted results and drafted the manuscript.

Funding

This work was partly supported by the Research Grants Council Theme-Based Research Scheme [T32-102-14N] and City University of Hong Kong [9610406, 7200548].

Acknowledgment

We thank all participants of the biweekly elder care project meetings for helpful comments and feedback. We thank all reviewers for the constructive comments which have helped us to substantially improve and clarify the manuscript.

Conflicts of interest

The authors declare no conflict of interest.

References

1. Yu L, Chan WM, Zhao Y *et al.* Personalized health monitoring system of elderly wellness at the community level in Hong Kong. *IEEE Access* 2018;**6**:35558–35567. doi:10.1109/ACCESS.2018.2848936.
2. Montgomery DC. Introduction to Statistical Quality Control. *John Wiley & Sons* 2007;7th Edition.

3. Waterhouse M, Smith I, Assareh H *et al.* Implementation of multivariate control charts in a clinical setting. *Int J Qual Health Care* 2010;**22**:408–414. doi:[10.1093/intqhc/mzq044](https://doi.org/10.1093/intqhc/mzq044).
4. Gan FF, Tang X, Zhu Y *et al.* Monitoring the quality of cardiac surgery based on three or more surgical outcomes using a new variable life-adjusted display. *Int J Qual Health Care* 2017;**29**:427–432. doi:[10.1093/intqhc/mzx033](https://doi.org/10.1093/intqhc/mzx033).
5. Harel O, Schisterman EF, Vexler A *et al.* Monitoring quality control. *Epidemiology* 2008;**19**:621–627. doi:[10.1097/ede.0b013e318176bfb2](https://doi.org/10.1097/ede.0b013e318176bfb2).
6. Woodall WH. The use of control charts in health-care and public-health surveillance. *J Qual Technol* 2006;**38**:89–104. doi:[10.1080/00224065.2006.11918593](https://doi.org/10.1080/00224065.2006.11918593).
7. Thor J, Lundberg J, Ask J *et al.* Application of statistical process control in healthcare improvement: systematic review. *Qual Saf Health Care* 2007;**16**:387–399. doi:[10.1136/qshc.2006.022194](https://doi.org/10.1136/qshc.2006.022194).
8. Tennant R, Mohammed MA, Coleman JJ *et al.* Monitoring patients using control charts: A systematic review. *Int J Qual Health Care* 2007;**19**:187–194. doi:[10.1093/intqhc/mzm015](https://doi.org/10.1093/intqhc/mzm015).
9. Ma FT, Lee CE. Integrated control chart for vital signs early warning of long-term care patients. *2014 7th International Conference on Ubi-Media Computing and Workshops* 2014;313–318. doi:[10.1109/U-MEDIA.2014.42](https://doi.org/10.1109/U-MEDIA.2014.42).
10. Cornélissen G, Halberg F, Hawkins D *et al.* Individual assessment of antihypertensive response by self-starting cumulative sums. *J Med Eng Technol* 1997;**21**:111–120. doi:[10.3109/03091909709031156](https://doi.org/10.3109/03091909709031156).
11. Sparks R, Cellar B, Okugami C *et al.* Telehealth monitoring of patients in the community. *J Intell Syst* 2016;**25**:37–53. doi:[10.1515/jisys-2014-0123](https://doi.org/10.1515/jisys-2014-0123)
12. Jones-Farmer LA, Ezell JD, Hazen BT. Applying control chart methods to enhance data quality. *Technometrics* 2014;**56**:29–41. doi:[10.1080/00401706.2013.804437](https://doi.org/10.1080/00401706.2013.804437).
13. Rigdon SE and Fricker RD. Health surveillance. In *ICSA Book Series in Statistics*, pages 203–249. Springer International Publishing, 2015. doi:[10.1007/978-3-319-18536-1_10](https://doi.org/10.1007/978-3-319-18536-1_10).
14. Gavish B, Ben-Dov IZ, Bursztyn M. Linear relationship between systolic and diastolic blood pressure monitored over 24 h: assessment and correlates. *J Hypertens* 2008;**26**:199–209. doi:[10.1097/HJH.0b013e3282f25b5a](https://doi.org/10.1097/HJH.0b013e3282f25b5a).
15. Needham DM, Sinopoli DJ, Dinglas VD *et al.* Improving data quality control in quality improvement projects. *Int J Qual Health Care* 2009;**21**:145–150. doi:[10.1093/intqhc/mzp005](https://doi.org/10.1093/intqhc/mzp005).
16. Celler B, Argha A, Varnfield M, *et al.* Patient adherence to scheduled vital sign measurements during home telemonitoring: analysis of the intervention arm in a before and after trial. *JMIR Med Inform* 2018;**6**:e15. doi:[10.2196/medinform.9200](https://doi.org/10.2196/medinform.9200).
17. Schafer JL, Graham JW. Missing data: our view of the state of the art. *Psychol Methods* 2002;**7**:147–177. doi:[10.1037/1082-989X.7.2.147](https://doi.org/10.1037/1082-989X.7.2.147).
18. Hebert PL, Taylor LT, Wang JJ *et al.* Methods for using data abstracted from medical charts to impute longitudinal missing data in a clinical trial. *Value Health* 2011;**14**:1085–1091. doi:[10.1016/j.jval.2011.05.049](https://doi.org/10.1016/j.jval.2011.05.049).
19. Madbuly DF, Maravelakis PE, Mahmoud MA. The effect of methods for handling missing values on the performance of the MEWMA control chart. *Commun Stat Simul Comput* 2013;**42**:1437–1454. doi:[10.1080/03610918.2012.665547](https://doi.org/10.1080/03610918.2012.665547).
20. Mahmoud MA, Saleh NA, Madbuly DF. Phase I analysis of individual observations with missing data. *Qual Reliab Eng Int* 2014;**30**:559–569. doi:[10.1002/qre.1508](https://doi.org/10.1002/qre.1508).

21. Penny KI, Atkinson I. Approaches for dealing with missing data in health care studies. *J Clin Nurs* 2012;**21**:2722–2729. doi:10.1111/j.1365-2702.2011.03854.x.
22. Huang W, Shu L, Woodall WH *et al.* CUSUM procedures with probability control limits for monitoring processes with variable sample sizes. *IIE Trans* 2016;**48**:759–771. doi:10.1080/0740817x.2016.1146422.
23. Aslam M, Arif OH, Jun, CH. A new variable sample size control chart using MDS sampling. *J Stat Comput Simul* 2016;**86**:3620–3628. doi:10.1080/00949655.2016.1178263.
24. Aparisi F. Hotelling's T^2 control chart with adaptive sample sizes. *Int J Prod Res* 1996;**34**:2853–2862. doi:10.1080/00207549608905062.
25. Kim K, Reynolds Jr MR. Multivariate monitoring using an MEWMA control chart with unequal sample sizes. *J Qual Technol* 2005;**37**:267–281. doi:10.1080/00224065.2005.11980330.
26. Alfaro JL, Ortega JF. A comparison of robust alternatives to Hotelling's T^2 control chart. *J Appl Stat* 2009;**36**:1385–1396. doi:10.1080/02664760902810813.
27. Maronna RA, Zamar RH. Robust estimates of location and dispersion for high-dimensional datasets. *Technometrics* 2002;**44**:307–317. doi:10.1198/004017002188618509.
28. Todorov V, Filzmoser P. An object-oriented framework for robust multivariate analysis. *J Stat Softw* 2009;**32**:1–47. doi:10.18637/jss.v032.i03.
29. Mason RL, Tracy ND, Young JC. Decomposition of T^2 for multivariate control chart interpretation. *J Qual Technol* 1995;**27**:99–108. doi:10.1080/00224065.1995.11979573.
30. Mardia KV. Measures of multivariate skewness and kurtosis with applications. *Biometrika* 1970;**57**:519–530. doi:10.1093/biomet/57.3.519.
31. Henze N, Zirkler B. A class of invariant consistent tests for multivariate normality. *Commun Stat Theory Methods* 1990;**19**:3595–3617. doi:10.1080/03610929008830400.
32. Korkmaz S, Goksuluk D, Zararsiz G. MVN: An R package for assessing multivariate normality. *R J* 2014;**6**:151–162. doi:10.32614/RJ-2014-031.
33. Hryniewicz O, Kaczmarek-Majer K. Monitoring of non-stationary health-recovery processes with control charts. *Int J Adv Life Sci* 2018;**10**:31–41.
34. Bartlett MS. The Effect of standardization on a χ^2 approximation in factor analysis. *Biometrika* 1951;**3**–**4**:337–344. doi:10.1093/biomet/38.3-4.337.
35. Brewster L, Mountain G, Wessels B *et al.* Factors affecting front line staff acceptance of telehealth technologies: a mixed-method systematic review. *J Adv Nurs* 2013;**70**:21–33. doi:10.1111/jan.12196.
36. Taylor J, Coates E, Brewster L *et al.* Examining the use of telehealth in community nursing: identifying the factors affecting frontline staff acceptance and telehealth adoption. *J Adv Nurs* 2014;**71**:326–337. doi:10.1111/jan.12480.
37. Celler BG, Sparks RS. Home telemonitoring of vital signs—technical challenges and future directions. *J Biomed Inform* 2015;**19**:82–91. doi:10.1109/jbhi.2014.2351413.

Appendix

In this appendix, we provide the derivation of the adjustment factor \mathbf{W}_i as used in equation (1): $\Sigma_{\bar{\mathbf{x}}_i} = \mathbf{W}_i \odot \Sigma$. As stated in equation (2), \mathbf{W}_i is equal to

$$\mathbf{W}_i = \left[\frac{|U_{ij} \cap U_{ij'}|}{n_{ij}n_{ij'}} \right]_{j,j'=1,\dots,p}.$$

As discussed in section 2.4, U_{ij} is the set of elders who showed up for measuring their vital sign j on day i and define $n_{ij} = |U_{ij}|$. Recall that the matrix $\Sigma_{\bar{\mathbf{X}}_i}$ is the covariance matrix for the random mean vector $\bar{\mathbf{X}}_i$ which is defined as

$$\bar{\mathbf{X}}_i = \left[\frac{1}{n_{ij}} \sum_{k \in U_{ij}} X_{ijk} \right]_{j=1, \dots, p}.$$

Following a similar set-up as [25], we derive the covariance between any two elements j and j' of $\bar{\mathbf{X}}_i$ as

$$\begin{aligned} \text{Cov}(\bar{X}_{ij}, \bar{X}_{ij'}) &= \text{Cov} \left(\frac{1}{n_{ij}} \sum_{k \in U_{ij}} X_{ijk}, \frac{1}{n_{ij'}} \sum_{k' \in U_{ij'}} X_{ij'k'} \right) \\ &= \frac{1}{n_{ij}n_{ij'}} \sum_{k \in U_{ij}} \sum_{k' \in U_{ij'}} \text{Cov}(X_{ijk}, X_{ij'k'}). \end{aligned}$$

We assume independence of observations between individual elder, i.e., $\text{Cov}(X_{ijk}, X_{ij'k'}) = 0$ whenever $k \neq k'$. Now it follows that

$$\begin{aligned} \text{Cov}(\bar{X}_{ij}, \bar{X}_{ij'}) &= \frac{1}{n_{ij}n_{ij'}} \sum_{k \in U_{ij} \cap U_{ij'}} \text{Cov}(X_{ijk}, X_{ij'k}) \\ &= \frac{|U_{ij} \cap U_{ij'}|}{n_{ij}n_{ij'}} \text{Cov}(X_{ij}, X_{ij'}) \\ &= \frac{|U_{ij} \cap U_{ij'}|}{n_{ij}n_{ij'}} \sigma_{jj'}. \end{aligned}$$

Alternatively, we can write

$$\Sigma_{\bar{\mathbf{X}}_i} = \left[\frac{|U_{ij} \cap U_{ij'}|}{n_{ij}n_{ij'}} \sigma_{jj'} \right]_{j, j'=1, \dots, p}.$$

Where $\mathbf{W}_i = [|U_{ij} \cap U_{ij'}| / n_{ij}n_{ij'}]$, can be interpreted as the weighting matrix which takes the number of observed data points into account. Hence, the covariance matrix of $\bar{\mathbf{X}}_i$ is equal to

$$\Sigma_{\bar{\mathbf{X}}_i} = \mathbf{W}_i \odot \Sigma$$

where, \odot is the Hadamard product, which denotes element wise matrix multiplication and Σ is the covariance matrix of the individual data.